Near-field second-harmonic generation in single gold nanoparticles

M. Zavelani-Rossi,[1,a)] M. Celebrano,[1] P. Biagioni,[1] D. Polli,[1] M. Finazzi,[1] L. Duò,[1] G. Cerullo,[1] M. Labardi,[2] M. Allegrini,[2] J. Grand,[3] and P.-M. Adam[3]
[1]*Dipartimento di Fisica, Politecnico di Milano, piazza L. da Vinci 32, 20133 Milano, Italy*
[2]*INFM-CNR PolyLab, Dipartimento di Fisica "Enrico Fermi," Università di Pisa, Largo B. Pontecorvo 3, 56127 Pisa, Italy*
[3]*Laboratoire de Nanotechnologie et d'Instrumentation Optique, Université de Technologie de Troyes, 12 Rue Marie Curie, 10010 Troyes, France*

(Received 16 October 2007; accepted 8 February 2008; published online 6 March 2008)

Second-harmonic generation from single gold elliptical nanoparticles is experimentally investigated by a nonlinear scanning near-field optical microscope (SNOM). The near-field nonlinear response is found to be directly related to local surface plasmon resonances and to particle morphology. The combined analysis of linear and second-harmonic SNOM images provides discrimination among different light extinction particle behaviors, not achievable just with linear techniques. The polarization state of the emitted second harmonic is also investigated, providing experimental evidence of second-harmonic particle emission modes peculiar to near-field excitation. © *2008 American Institute of Physics*. [DOI: 10.1063/1.2889450]

The explosive growth of nanoscience and nanotechnology during the past decade has led to great interest in the investigation of nanoscale optical fields and to the development of tools for their study.[1] One of the most remarkable effects in light interaction with metal nanostructures is the strong and spatially localized field amplitude enhancement, due to lightning rod effects induced by the sharp curvatures[1] and/or to resonant excitation of localized surface plasmons (LSPs) in single or coupled particles.[2,3] LSP resonance frequencies can be tailored in a broad spectral range according to the material and shape of the nanostructure. Conventional far-field techniques, such as confocal microscopy, can address the average optical properties of nanoparticle arrays but they are limited by diffraction and do not provide topographic information. On the other hand, scanning near-field optical microscopy (SNOM) allows beating the diffraction limit by confining light on the nanoscale and enables to single out the optical response of an individual nanostructure in high density arrangements, simultaneously acquiring a topographic map. The nature of near-field illumination is inherently different from that of usual propagative waves, enabling the observation and exploitation of unusual and peculiar light-interaction modes.

SNOM imaging of metal nanostructures at the fundamental wavelength (FW) results from an intricate combination of linear processes, such as scattering, absorption, and reflection, all contributing to light extinction.[1] Thus, drawing a simple relation between FW contrast and particle behavior may sometimes not be an easy task. The particle properties can be better understood by exploiting the additional information given by the nonlinear optical response. Second order effects, such as second-harmonic generation[4–9] (SHG) and two-photon photoluminescence (TPPL),[10–12] which depend on the square of the light intensity, are very sensitive probes of local field enhancements. A number of theoretical studies have addressed SHG response of nanostructured systems.[13–16] Experimental investigations have been performed with SNOM and far-field confocal microscopy on rough metal surfaces,[4–7] where the relationship between SHG and LSP frequencies could just be inferred, or on nanofabricated metal particles, both isolated[8] or in high density patterns.[9]

In this work, we use a nonlinear aperture SNOM providing polarized high-peak-intensity femtosecond light pulses in the near-field to study SHG from single gold nanoparticles. Near-field SHG reveals local field enhancements, due to both LSP resonances and particle nanomorphology, with high spatial resolution (less than 100 nm) and sensitivity. Discrimination among different light extinction particle behaviors, not achievable with just linear techniques, is obtained by a combined analysis of linear and SH SNOM images.

In our setup, we couple femtosecond pulses to an aperture SNOM based on a hollow pyramid tip. The 30 fs, 800 nm pulses are generated by a stretched cavity Ti:sapphire oscillator (26 MHz repetition rate).[9] The silicon nitride tip is aluminum-coated with a circular aperture at the apex,[17] with diameter ranging between 100 and 200 nm. These probes have high throughput, low absorption, preserve light polarization,[18] and do not introduce chirping for pulses as short as 30 fs.[19] Typical tip throughputs at 800 nm range between $\sim 10^{-4}$ for the 100 nm tips and $\sim 5 \times 10^{-3}$ for the 200 nm ones. The optical signals are collected in the far field in transmission geometry by a 0.75 NA long-working-distance microscope objective and suitably filtered in order to separate with high rejection ratio the SH from both FW (which is recorded separately) and TPPL, which is negligible for wavelength shorter than 450 nm.[2,11,20] The quadratic dependence of SH intensity on the excitation beam power was verified.

Figure 1 shows SNOM images from gold nanoparticles produced by electron beam lithography on a quartz substrate and arranged in square arrays.[2] The particle height is ~60 nm, the minor axis is ~70 nm long, the major axes are ~100, 150 or 400 nm long and the array period is 1 μm. Far-field extinction spectra, with exciting white light polarization parallel to the major axis, display a LSP resonance centered around 690 nm for the 100 nm particles, around 800 nm (i.e., resonant with our FW) for the 150 nm ones and above 1000 nm for the 400 nm ones. In Fig. 1 we show

a)Author to whom correspondence should be addressed. Electronic mail: margherita.zavelani@fisi.polimi.it.

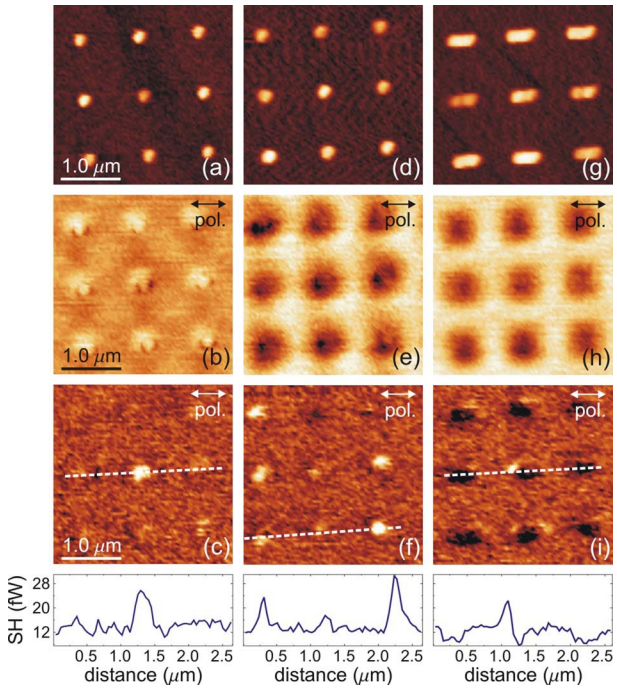

FIG. 1. (Color online) Nanoparticles: [(a), (d) and (g)] topography, [(b), (e) and (h)] FW transmission, [(c), (f) and (i)] SH emission SNOM images with corresponding cross sections along the dashed lines, from the raw data. Incident light is polarized parallel to the major axis. Major axis length: 100 nm [(a)–(c)], 150 nm [(d)–(f)], 400 nm [(g)–(i)]. Image size: 3×3 μm^2.

topography [(a), (d), and (g)], FW SNOM transmission [(b), (e), and (h)], and SH SNOM emission [(c), (f), and (i)] of the different nanoparticles, obtained by a 200 nm aperture and incident light polarization along the major axis. The optical images at both FW and SH wavelengths strongly depend on the particle size, and show three qualitatively different interaction regimes.

A possible explanation for the behavior of the 100 nm particles might be that they appear bright in the FW maps because of a redshift of their LSP resonance induced by the presence of the SNOM tip. However, this is not consistent with SH maps, where the particles do not emit significant SH radiation, as expected from nonresonant particles.[2] A more likely interpretation can be given in terms of near-field scattering, which might even reduce the light extinction. Clear signs of interference and near-field diffraction effects[21] can also be noticed, since the spatial periodicity of the particles is close to our excitation wavelength. The FW map of the 150 nm particles is in agreement with far-field extinction spectra. They appear dark with high contrast because the excitation energy is set at the LSP resonance. A uniform emission of relatively intense SH (see cross sections in Fig. 1) by most of the particles is observed as a result of LSP field enhancement.[20] Finally, the 400 nm particles strongly absorb/reflect both the FW and the background SH generated by the tip, as evident since they appear darker than the substrate. Indeed, in this case the size of the particle is larger than the aperture. We can exclude that the qualitative differences observed in the SH maps displayed in Fig. 1 might be due to the scattering of the SH field emitted directly by the tip itself since the particles do not display either LSP resonance[2] or intraband transitions[22] at the SH frequency and their radius of curvature at the apex, defining possible lightning-rod effects, appears as fairly constant in the topographic maps regardless of the length of the particle.

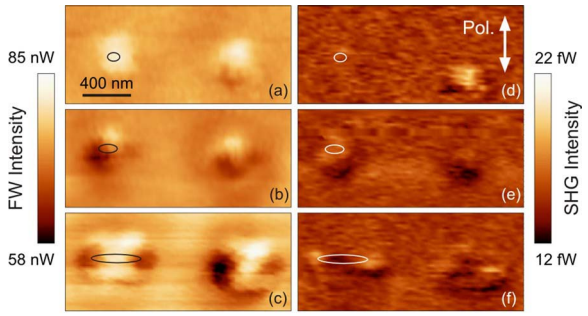

FIG. 2. (Color online) [(a)–(c)] FW transmission and [(d)–(f)] SH emission excited by incident FW light polarized perpendicular to the particle major axis. The particle major axis is 100 nm [(a) and (d)], 150 nm [(b) and (e)], and 400 nm [(c) and (f)].

A remarkable feature in Fig. 1 is the strong variability of the SHG efficiency. Indeed, nominally identical particles display quite similar FW signals, but, in some cases, very different SH ones. The absence of a strict correlation between the topography and either the FW or SH intensity maps is a clear indication of the absence of relevant topographic artifacts in the optical images.[8] In particular, (i) particles that more strongly emit SH appear dark in FW images and (ii) not all the particles appearing dark in FW maps also exhibit SH emission. These observations are in agreement with the theoretical predictions of Refs. 15 and 16. We explain the correlation between extinction and SHG as follows: (i) resonance with the nanoparticle LSP and/or lightning rod effects in areas with high curvature or local imperfections ("hot spots") give rise to a strong field enhancement, (ii) SH can be efficiently generated only in presence of such an enhancement,[2,20,22] which (iii) also increases FW absorption/scattering, resulting in a higher extinction in the FW maps. Thus, the SHG efficiency depends on the particle fine structure, which determines local field enhancements, mainly induced by both LSP excitation and lightning rod effects. This is also evident in the SH images of some of the nonresonant 400 nm particles [Fig. 1(i)], where generation occurs when exciting at the particle edges due to localized high curvatures.

SHG dependence on LSP is further highlighted in Fig. 2, showing optical images obtained by using a 100 nm aperture and an excitation light polarized parallel to the minor axis of the particles. In this case, both 100 and 150 nm particles are off resonance. Similar to the nonresonant 100 nm particles shown in Fig. 1, they appear bright in the FW maps and do not emit SH radiation, in agreement with the interpretation given above. SH emission can just be observed at some sites due to local imperfections. On the other hand, the dark FW and bright SH spots visible on the 400 nm particles in Figs. 2(c) and 2(f) show that, with polarization parallel to the particle minor axis, these particles resonate when illuminated at the edges. This behavior is coherent with the generally observed complementarity between the FW and SH maps.

The SH SNOM has two main peculiarities compared to the linear one. The first is an effective background rejection in the SH maps, resulting in improved image contrast, which can be even increased using a polarizer on detection, as it will be clear in the next paragraphs. The second is an enhanced resolution (less than 100 nm), which goes beyond the factor of $\sqrt{2}$ expected between SH and FW intensity distri-

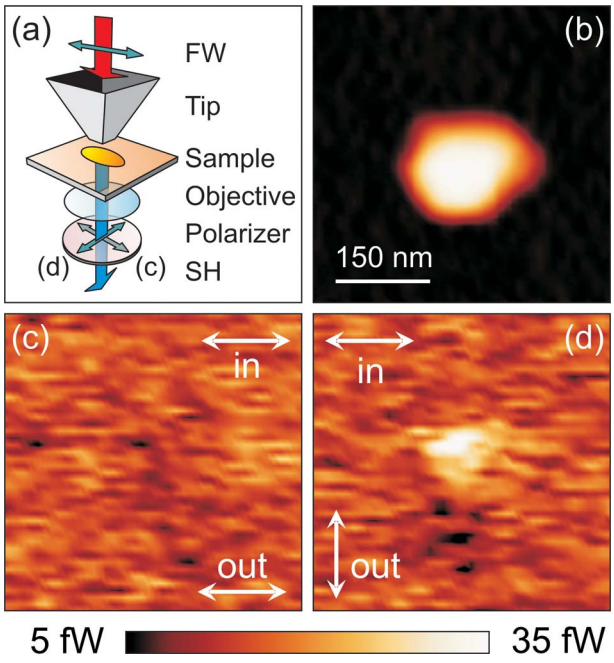

FIG. 3. (Color online) Polarization of the SH generated by nanoparticles with 150 nm major axis: (a) experimental geometry (the FW light is polarized parallel to the particle major axis), (b) topography, [(c) and (d)] SH emission map with a polarizer on detection parallel (c), and perpendicular (d) to the particle major axis. Image size: $0.45 \times 0.45\ \mu m^2$.

butions. Such high resolution could be ascribed to a tip-on-aperture field enhancement mechanism,[23] where the role of the aperture is to convey energy to a sharp protrusion of the metal coating that acts as a near-field scattering center.

The polarization state of the SH light emitted by the gold nanoparticles was analyzed by a polarizer on detection. Figure 3 shows two typical SH maps of a 150 nm particle excited with FW light impinging into the tip with polarization parallel to the particle major axis, with the polarizer parallel [Fig. 3(c)] or perpendicular [Fig. 3(d)] to the FW excitation field [see Fig. 3(a) for a sketch of the experimental geometry]. The emitted SH light from all the particles that we have analyzed is strongly polarized [see Figs. 3(c) and 3(d)]. This is a remarkable result since, according to the selection rules discussed in Ref. 24, the FW component polarized parallel to the plane of the sample gives rise to a SH dipole oriented orthogonal to the substrate. The corresponding SH emission pattern has cylindrical symmetry around the substrate normal and, consequently, would not show any dependence upon the analyzer orientation. The only possibility to have a SH pattern displaying the observed polarization dependence is to have an emitting SH dipole in the plane of the substrate. The excitation of such a dipole requires a significant contribution from the longitudinal (parallel to the tip axis) component of the FW field. Such a component is indeed characteristic of near-field excitation. In particular, the polarization dependence shown in Fig. 3 indicates SH emission from an electric dipole oriented along the particle minor axis [Fig. 3(a)]. The reason why such a mode prevails on other allowed SH dipole emission channels resides in the details of the particle geometry. Theoretical modeling of metal nanostructures observed by far-field[16] and near-field[14] microscopy has shown that polarized SH emission might have a complex dependence on particle shape and resonance conditions. Also, symmetry breaking might play an important role.[24,25] Here, we tentatively attribute the prevailing contribution of SH light oriented parallel to the particle minor axis to the larger portion of gold/air interface available along the long sides of the particles. This explanation is supported by the fact that an interface locally breaks the inversion symmetry of the bulk and therefore represents a source of SH radiation

In conclusion, we have shown that SHG on the nanoscale provides unique information on the local field enhancement distribution with respect to conventional linear SNOM and far-field microscopy. In particular, near-field SHG is shown to be very sensitive to LSP resonances as well as to the morphology of the nanostructures. The complementarity of near-field FW and SH maps allows to reliably evaluate intensity distributions and to address near-field scattering/absorption and emission processes. Finally, analysis of the polarization state of the emitted SH gives a clear signature of SH emission modes peculiar to near-field excitation.

[1] L. Novotny and B. Hecht, *Principles of Nano-Optics* (Cambridge University Press, New York, 2006).
[2] J. Grand, S. Kostcheev, J.-L. Bijoeon, M. L. de la Chapelle, P.-M. Adam, A. Rumyantseva, G. Lérondel, and P. Royer, Synth. Met. **139**, 621 (2003).
[3] P. Mühlschlegel, H.-J. Eisler, O. J. F. Martin, B. Hecht, and D. W. Pohl, Science **308**, 1607 (2005).
[4] I. I. Smolyaninov, A. V. Zayats, and C. C. Davis, Phys. Rev. B **56**, 9290 (1997).
[5] A. V. Zayats, T. Kalkbrenner, V. Sandoghdar, and J. Mlynek, Phys. Rev. B **61**, 4545 (2000).
[6] S. I. Bozhevolnyi, J. Beermann, and V. Coello, Phys. Rev. Lett. **90**, 197403 (2003).
[7] C. Anceau, S. Brasselet, J. Zyss, and P. Gadenne, Opt. Lett. **28**, 713 (2003).
[8] M. Breit, S. Malkmus, J. Feldmann, and H. U. Danzebrink, Appl. Phys. Lett. **90**, 093114 (2007).
[9] M. Celebrano, M. Zavelani-Rossi, D. Polli, G. Cerullo, P. Biagioni, M. Finazzi, L. Duò, M. Labardi, M. Allegrini, J. Grand, and P.-M. Adam, J. Microsc. **229**, 233 (2008).
[10] A. Bouhelier, M. R. Beversluis, and L. Novotny, Appl. Phys. Lett. **83**, 5041 (2003).
[11] A. Bouhelier, R. Bachelot, G. Lerondel, S. Kostcheev, P. Royer, and G. P. Wiederrecht, Phys. Rev. Lett. **95**, 267405 (2005).
[12] K. Imura, T. Nagahara, and H. Okamoto, J. Phys. Chem. B **109**, 13214 (2005).
[13] J. I. Dadap, J. Shan, K. B. Eisenthal, and T. F. Heinz, Phys. Rev. Lett. **83**, 4045 (1999).
[14] S. I. Bozhevolnyi and V. Z. Lozovski, Phys. Rev. B **61**, 11139 (2000); **65**, 235420 (2002).
[15] M. I. Stockman, D. J. Bergman, C. Anceau, S. Brasselet, and J. Zyss, Phys. Rev. Lett. **92**, 057402 (2004).
[16] J. Beermann, S. I. Bozhevolnyi, and V. Coello, Phys. Rev. B **73**, 115408 (2006).
[17] S. Werner, O. Rudow, C. Mihalcea, and E. Oesterschulze, Appl. Phys. A: Mater. Sci. Process. **66**, 367 (1998).
[18] P. Biagioni, D. Polli, M. Labardi, A. Pucci, G. Ruggeri, G. Cerullo, M. Finazzi, and L. Duò, Appl. Phys. Lett. **87**, 223112 (2005).
[19] M. Labardi, M. Zavelani-Rossi, D. Polli, G. Cerullo, M. Allegrini, S. De Silvestri, and O. Svelto, Appl. Phys. Lett. **86**, 031105 (2005).
[20] C. Hubert, L. Billot, P.-M. Adam, R. Bachelot, P. Royer, J. Grand, D. Gindre, K. D. Dorkenoo, and A. Fort, Appl. Phys. Lett. **90**, 181105 (2007).
[21] Th. Huser, L. Novotny, Th. Lacoste, R. Eckert, and H. J. Heinzelmann, J. Opt. Soc. Am. B **16**, 141 (1999).
[22] The SH signal cannot be assigned to interband transitions, which are around 550 nm for gold, i.e., far away from the excitation energy of the laser beam at both the FW and the SH, and would provide a response which does not depend on particle shape.
[23] H. G. Frey, F. Keilmann, A. Kriele, and R. Guckenberger, Appl. Phys. Lett. **81**, 5030 (2002).
[24] M. Finazzi, P. Biagioni, M. Celebrano, and L. Duò, Phys. Rev. B **76**, 125414 (2007).
[25] S. Kujala, B. K. Canfield, M. Kauranen, Y. Svirko, and J. Turunen, Phys. Rev. Lett. **98**, 167403 (2007).